Development of focusing grating couplers for lithium niobate on insulator platform

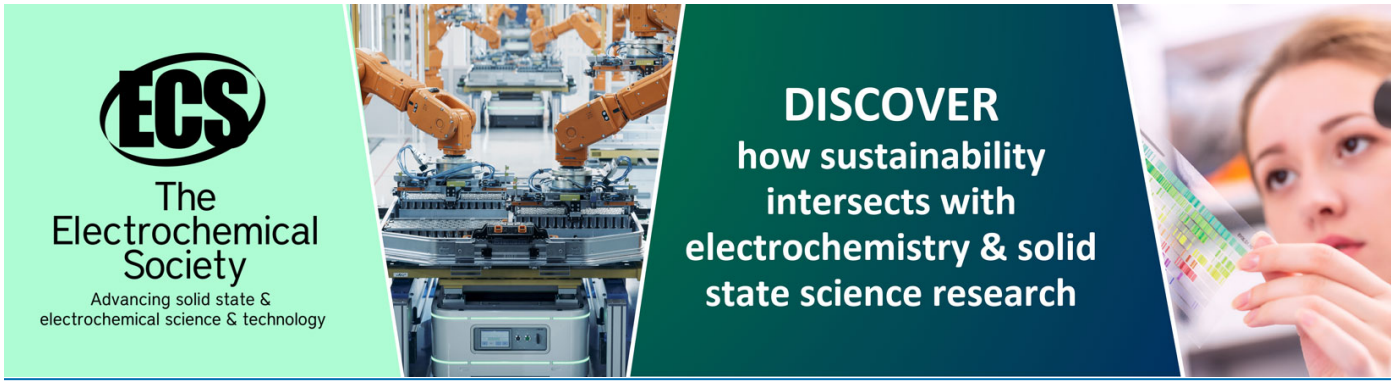

Development of focusing grating couplers for lithium niobate on insulator platform

I Elmanov[1], F Sardi[2], K Xia[2], T Kornher[2], V Kovalyuk[1,3], A Prokhodtsov[1,4], P An[1,3], A Kuzin[1,5], A Elmanova[1], G Goltsman[1,3,4], R Kolesov[2]
[1]Department of Physics, Moscow State Pedagogical University, Russia
[2]3rd Institute of Physics, University of Stuttgart, Germany
[3]Zavoisky Physical-Technical Institute of the Russian Academy of Sciences, Russia
[4]National Research University Higher School of Economics, Moscow, Russia
[5]Skolkovo Institute of Science and Technology, 121205, Russia

Abstract. In this paper, we fabricate and experimentally study focusing grating couplers for lithium niobate on an insulator photonic platform. The transmittance of a waveguide equipped with in- and out- couplers with respect to the grating period is measured with and without silicon dioxide cladding applied. Our results show the influence of silicon dioxide cladding on the efficiency and the central wavelength of grating couplers and can be used to improve grating coupling efficiency. Our study is supported by numerical simulations.

1. Introduction

Lithium niobate on insulator (LNOI) is a promising platform for different scalable on-chip devices offering nonlinear wavelength conversion and high-speed modulation of light [1]. Such properties of the material as high refractive index, large second-order nonlinear susceptibility and wide optical transparency range are very remarkable in the field of photonics and were mentioned in recent works about various optical devices, such as tunable ring resonators [2], low-loss waveguides [3] and optical modulators [4]. This platform can also be used for integrated photonic circuits [5]. Today it is an important task to provide a way of integration of on-chip devices with optical fibers. One of the challenges is efficient in- and out-coupling of light into and out of planar on-chip photonic circuits. Focusing grating couplers (FGCs) are potentially a highly efficient way of extracting light from planar optical structures. They can be used for LNOI structures [6] similar to silicon-on-insulator (SOI) ones [7]. However, their fabrication and development is a challenging task due to rather hard processing of LN by wet or dry etching. Here, we present our first preliminary results on in- and out-coupling of light by means of FGCs created by reactive ion etching. In our work we develop FGCs on LNOI platform for telecommunication wavelength 1550 nm, study the influence on its properties of a protective silicon dioxide cladding.

2. Device design and fabrication

For LNOI coupler development, we optimized the geometry of FGC demonstrated for SOI [8]. A single nanophotonic circuit included two FGCs connected by a 900 nm wide ridge waveguide (Figure 1 a, c). For a detailed study of FGC, we created an array of devices with grating periods varying in the range of 800 - 900 nm with the fixed filling factor 0.5. For the device fabrication we used commercially available lithium niobate on insulator wafers (NanoLN) with 470 nm thick lithium niobate film residing on a silicon wafer with 2 μm SiO_2 spacer. The fabrication process was realized by e-beam lithography using

double-layer PMMA as a positive e-beam resist. The top PMMA layer (thickness 80 nm) with 950K molecular weight was put on top of a more sensitive 200 K layer (thickness 400 nm). This facilitates the undercut of the developed structures and promotes smooth lift-off of the hard metal mask. After the e-beam writing is completed and PMMA structures are developed with MIBK developer, 120 nm thick nichrome (50/50 Ni/Cr) hard mask was deposited by e-gun evaporation. Lift-off of the hard mask was performed in warm N-ethyl pyrrolidone. Lithium niobate structures were then produced by etching $LiNbO_3$ through the nichrome mask in an Ar/SF_6 low-pressure plasma with no ICP component. After etching, the residual nichrome mask was removed in a mixture of chromium etchant and nitric acid. Final structures have 70° sidewall angle, as it normally occurs when LN passes throw reactive ion etching [9] (Figure 1 (b, c)). After fabrication and first measurements of all devices, the chip was covered by a 1 μm thick silicon dioxide layer.

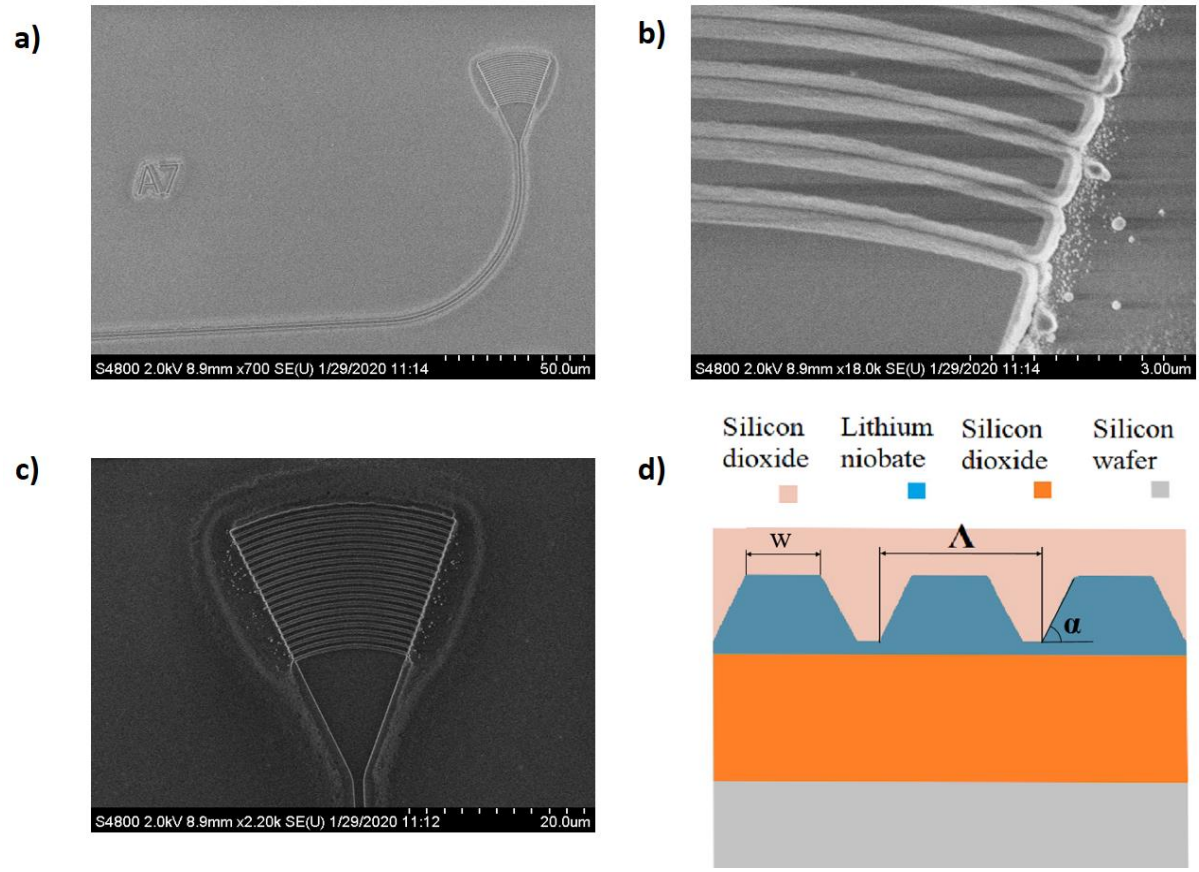

Figure 1(a-d). (a) SEM image of a fabricated structure. The second grating coupler is on the left out of the SEM field of view. The distance between the grating couplers matches the spacing between the fibers of the 12-channel array (see text); **(b, c)** SEM image of a fabricated focusing grating coupler; **(d)** Schematic image of cross-section of a FGC, where Λ is the grating coupler period, w is a tooth width, filling factor $ff = w/\Lambda$, α is an angle of a tooth's side inclination.

3. Experimental results

For the experimental study we used a tunable laser source (New Focus TLB-6600) covering the wavelength range of 1510÷1620 nm and having an optical power of 1 mW. It is optically connected to a single-mode 12-channel fiber array (FA) and polarization controller with a chip placed on top of a *x*, *y*, *z*, rotation piezo stage. The stage allowed for the alignment of the two neighbouring fibers in the array on top of the grating couplers belonging to the same waveguide. One fiber was used to inject light while the other was used to collect light at the output port. Transmission spectra of the devices were measured

by a fast photodetector and, after preliminary amplification of the electrical signal, were registered by NI DAQ system. Several measured transmission spectra of nanophotonic devices from the array are shown in Figure 2. It can be seen that with an increase in the period of the grating, the maximum intensity moves to higher wavelengths (Figure 2 (a)). Nevertheless, the main Gaussian transmission spectra are outside the tunability range of our laser source. The 1 μm SiO_2 coating increases the effective refractive index, but nonetheless, is not sufficient to shift the maximum to the required wavelength of 1.55 μm. (Figure 2 (b)). Although, the central wavelength shifts to greater values due to SiO_2 cladding, the cladding decreases total coupling efficiency. The maximum coupling efficiency for 1.55 μm wavelength was found to be ≈ - 17 dB for the 900 nm grating period. These results required some simulation of our FGCs for a better estimation of a grating period for the wavelength of interest.

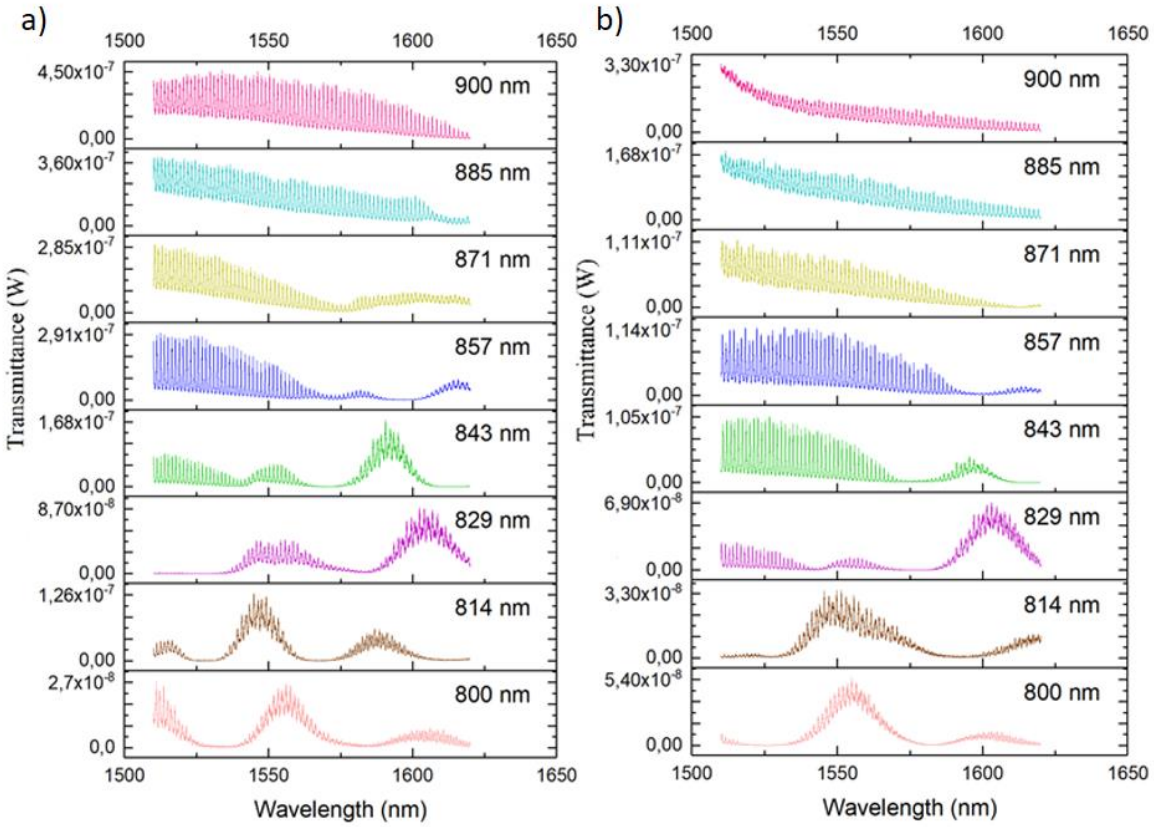

Figure 2(a, b). Transmission spectra for different grating periods before **(a)** and after silicon oxide sputtering **(b)**.

4. Simulation

For simulation, we used a 2D model of a FGC and a cross-section of a straight waveguide. We used a model with inclined sidewalls and non-fully etched LN. The etching depth was chosen to be 450 nm with the sidewall angle being 60° for FGC's grating teeth and 71 degrees for the straight waveguide. Numerical computation was performed using the finite element method (FEM) with COMSOL Multiphysics software. TE mode was calculated for straight LN waveguide before and after silicon dioxide sputtering as shown in Figure 3 (a, b).

Figures 3 (c, d) show the normalized electric field corresponding to the wavelength of 1550 nm for a side view of an FGC with lithium niobate on a silicon substrate having a period of 900 nm and a filling factor of 0.5. The simulated structure mimics the produced devices. Both cladded and uncladded cases were considered. In the model, only the real part of the refractive index was specified, therefore, the

effective index of the gratings is slightly overestimated. The optical field was injected from above the gratings using a Gaussian beam with an 8° angle of incidence.

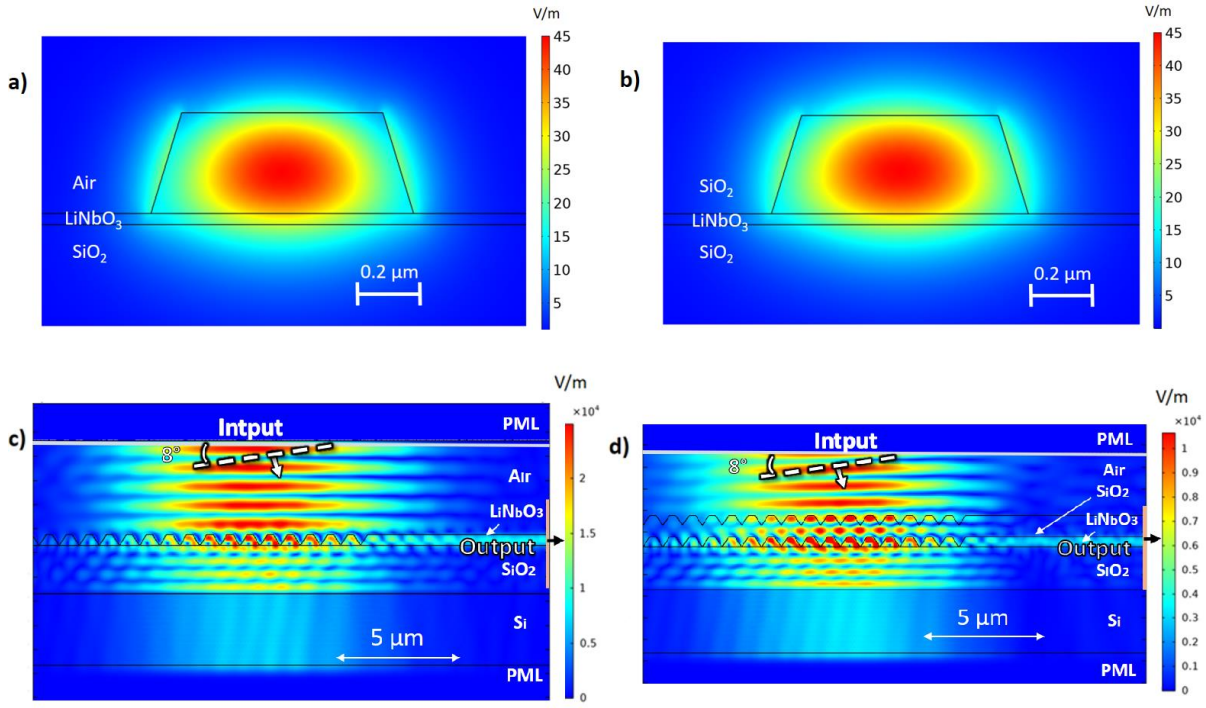

Figure 3. Simulated mode field distributions in the waveguide before **(a)** and after silicon oxide **(b)** sputtering; The normalized electric field propagation in a model without silicon oxide coating when the Gaussian beam is incident at 8°to the normal **(c)** and with silicon oxide **(d)**.

The beam size was approximately equal to the diameter of the optical fiber. To decrease the effect of reflection from the boundaries of the models, the Perfectly Matched Layer (PML) was used. The shape of the SiO_2 coating varied following the geometry of the lithium niobate layer and thickness equal to 1 µm throughout the entire length of lithium niobate (Figure 3 (d)).

Figure 4 shows the dependencies of the transmission spectra on the wavelength for the two models shown in Figure 3 (c, d). The blue simulation curves were calculated as the square of the absolute value of the normalized transmission component. The obtained simulation data were approximated using Gaussian fitting functions. The experimental transmission data for a period of 900 nm (Figure 2) were normalized to an input power of 1 mW. This plot clearly shows the redshift of central maximum transmittance wavelength upon cladding the LN structure with silica.

5. Discussion

A comparison of the experimental results and simulations proves our assumption of the real position of the main Gaussian transmission spectra and the influence of a silicon dioxide cladding on its position. Also, the present model provides us with a quantitative result about the main FGC parameters (such as period and filling factor) required for the optimized fabrication of FGCs operating at 1550 nm wavelength. Using numerical simulation, we obtained a particular result for the presented model of the FGC with a silicon dioxide cladding. For placing of the central wavelength of transmission spectra at 1550 nm, we should have a period of the FGC equal to about 950 nm and a filling factor equal to 0.5. Even though the model is not replicating the behavior of the fabricated device, our comparison with experimental results indicates the right direction of the device optimization.

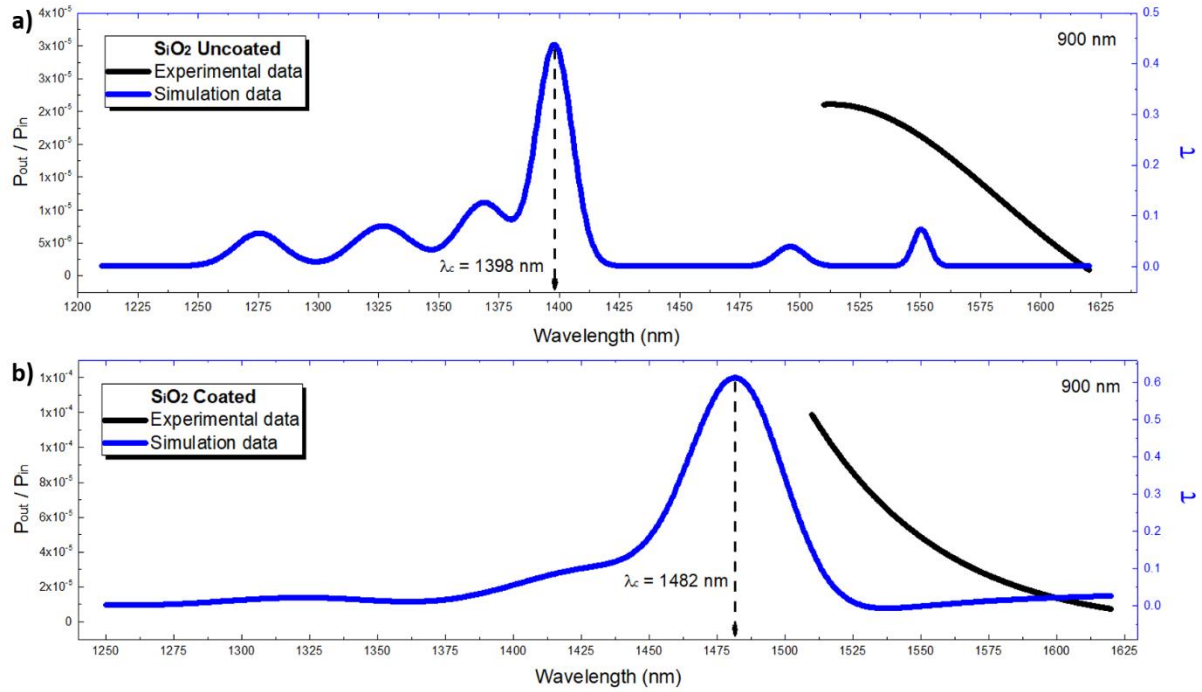

Figure 4(a-b). The black curve is the experimentally obtained data in the measurement range from 1510 to 1620 nm. The blue curve is the simulation data for transmission coefficient τ after fitting with Gauss functions (the imaginary part of the refractive index was not taken into account in the models, therefore the results are higher than the real ones); **(a)** Dependence of coupling efficiency on a linear scale on wavelength for a silica oxide-free model. The FGC period is 900 nm; the filling factor is 0.5. The maximum central wavelength for simulation data is at 1398 nm; **(b)** Dependence of coupling efficiency on a linear scale on wavelength for a silica model. The FGC period is 900 nm; the filling factor is 0.5. The silicon dioxide layer deposited on top is 1 micron. The maximum central wavelength for simulation data is at 1482 nm.

6. Conclusion

We studied the efficiency of FGCs depending on its period and application of a cladding layer of SiO_2 and determined ≈ -17 dB maximum coupling efficiency at 1.55 μm wavelength. A further increase of FGC's grating period with a fixed filling factor allows shifting the Gauss like transmission maximum closer to 1.55 μm wavelength, as shown in a numerical FEM simulation. Our results can be used for developing highly efficient coupling in and out of LNOI, which can be applied for the various quantum photonics devices, where compact design and high nonlinearity are needed simultaneously.

Acknowledgments

We acknowledge support of the Russian Science Foundation grant No. 19-72-10156 (experimental study), grant No. 16-12-00045 (numerical simulation), as well as grant No.17-72-30036 (theoretical study), Deutsche Forschungsgemeinschaft DFG KO4999/3-1 (nanoptotonic circuits fabrication).

References

[1] Zhang M, Wang C, Cheng R, Shams-Ansari A and Lončar M 2017 *Optica* **4** 1536–7
[2] Krasnokutska I, Tambasco J J and Peruzzo A 2019 *Sci Rep* **9** 11086
[3] Wu R, et al 2018 Low-loss Lithium Niobate on Insulator (LNOI) Waveguides of a 10 cm-length and a Sub-nanometer Surface Roughness *arXiv* arXiv:1810.09985
[4] Mercante A J, Shi S, Yao P, Xie L, Weikle R M and Prather D W 2018 *Opt. Express* **26** 14810–6

[5] Dutta S, Goldschmidt E A, Barik S, Saha U, Waks E 2019 An Integrated Photonic Platform for Rare-Earth Ions in Thin Film Lithium Niobate *arXiv* arXiv:1911.06376
[6] Krasnokutska I, Chapman R J, Tambasco J L J and Peruzzo A 2019 *Opt. Express* **27** 17681–5
[7] Vermeulen D, Selvaraja S, Verheyen P, Lepage G, Bogaerts W, Absil P, Van Thourhout D and Roelkens G 2010 *Opt. Express* **18** 278
[8] Van Laere F, Claes T, Schrauwen J, Scheerlinck S, Bogaerts W, Taillaert D, O'Faolain L, Van Thourhout D and Baets R 2007 *IEEE Photonics Tehnology Letters* **19** 1919–21
[9] Desiatov B, Shams-Ansari A, Zhang M, Wang C, Loncar M 2019 Ultra-low loss integrated visible photonics using thin-film lithium niobate *arXiv* arXiv:1902.08217